Properties of solid and gaseous hydrogen, based upon anisotropic pair interactions

R. D. Etters*
Colorado State University, Fort Collins, Colorado 80523

R. Danilowicz
Utica College, Utica, New York 13503

W. England
Argonne National Laboratory, Argonne, Illinois 60439

(Received 14 April 1975)

Properties of H_2 are investigated using an analytic anisotropic potential which has been deduced from recent atomic orbital and perturbation calculations. The low-pressure solid results are based upon a spherical average of the anisotropic potential. The calculated ground-state energy is $E_0 = -88.76 \pm 2$ K. The pressure-volume curve agrees with experiment to within 10% over the range $9 \leq V \leq 22.65$ cm^3/mole H_2. The high-pressure solid properties are calculated using the anisotropic potential for particular frozen orientations, as well as the spherically averaged potential. The structures investigated are the P_a3 and $P4_2/mnm$ orientations. The $P4_2/mnm$ orientation yields energies and pressures 10–20% lower than either the spherical average or the P_a3 arrangement. Agreement with experimental shock-wave data is tolerable. The metal-insulator phase-transition pressure is predicted to be between 1.61×10^6 and 3.76×10^6 atm, depending on the metallic equation of state used. Second virial coefficients $B(T)$ are calculated for H_2 and D_2 over the range 60 K $\leq T \leq$ 523 K, using a formalism which fully accounts for the potential anisotropies and the discrete rotational spectrum. The results are in excellent agreement with experiment except at high temperatures, where the discrepancy is nearly 10%. A comparison of the results with those obtained using the spherically averaged potential indicates that the effect of anisotropies on $B(T)$ is small. This coupled with the results from solid calculations implies that anisotropies are generally not very important except at extremely high pressures. The difference in $B(T)$ between ortho and para H_2 and D_2 is also calculated.

I. INTRODUCTION

There is no adequate theoretical description of many basic properties of molecular hydrogen. A central difficulty is the uncertainty in the H_2 pair interaction, which depends on the relative orientation of the two molecules. This anisotropy is a consequence of the nonspherical charge distribution. Nevertheless, it has been almost universally assumed that a spherically symmetric potential can well represent the system. This attitude is supported by the observation that the charge distribution departs from sphericity by only 8%.[1] There are several other reasons for ignoring anisotropies. First, techniques for predicting system properties, based upon anisotropic interactions, are complicated and poorly developed. Second, spherically symmetric, parametrized, semiphenomenological potential forms have been found which give calculated second virial coefficients in good agreement with experiment,[2] when the parameters are properly adjusted. A common example is the Lennard-Jones 6-12 potential. The problem is that when a potential so derived is used to calculate other system properties (viscosity, scattering cross sections, etc.), the results often agree badly with experiment. Generally, if the potential form and/or its parameters are selected to fit one set of experimental properties, other properties are poorly predicted.

A dramatic example of this failure is in the calculation of solid H_2 properties, based upon the 6-12 potential as deduced from second-virial-coefficient data.[2] Figure 1 shows the pressure-volume (PV) curve at zero temperature. The dashed line is based upon the 6-12 potential.[3] The circles and squares represent the experimental data.[4,5] As can be seen, agreement with experiment is not good, especially at higher pressures where the discrepancy approximates a factor of 2. Until recently, it was conjectured that this discrepancy was due to either poor experimental PV data or an inaccurate calculational procedure. These speculations are now largely disposed of because of recent experimental results of Anderson and Swenson[5] that support earlier work,[4] and by recent theoretical methods which have surmounted the difficulties in dealing with the large zero-point motion.[6] It is now apparent that inaccuracies greater than 10% in solid calculations must be attributed to a faulty potential representation.

A phenomenological potential that is quite different from the one deduced from second-virial-coefficient data has been unfolded from the cross-section measurements of Farrar and Lee.[7] Although the cross sections predicted using this po-

tential are in excellent agreement with experiment, the predicted second virial coefficients are very poor. Moreover, if this potential is used to calculate solid properties, such as the energy, PV, compressibility, etc., the agreement with experiment is also poor. These examples frame the problem.

We believe that the problems connected with molecular hydrogen (H_2) cannot be resolved using a phenomenological potential. Instead, we propose to investigate those theoretical calculations of the pair potential which are derived from first principles. From these data is deduced an analytic expression for the intermolecular potential which describes the interaction for arbitrary orientations of the molecules, without adjustable parameters, and where no *a priori* assumption is made regarding the anisotropy. A detailed analysis of various H_2 properties in the solid and gaseous phases, based upon this potential, is then presented. A recent note[8] gave a preliminary report on some of this work, although a somewhat different, not fully analytic, potential was used.[9]

II. THE POTENTIAL

Atomic orbital calculations of the potential are generally performed for four different relative orientations of the two molecules, called L, Π, X, and T. The L configuration corresponds to both intramolecular axes and the intermolecular axis along the same line. The Π configuration has both intramolecular axes parallel to one another and perpendicular to the intermolecular axis. The X configuration has all three axes perpendicular to one another, and the T configuration has one intramolecular axis parallel to the intermolecular axis and one perpendicular to it.

Arbitrary orientations are labeled according to Fig. 2, where θ_i and θ_j are the polar angles of molecules i and j with respect to the intermolecular axis of length $\vec{r}$. The associated azimuthal angles are ϕ_i and ϕ_j.

There are two different approaches used in these calculations. One method is to separate the potential into parts: the valence interaction U_V, which dominates at small separations and comes from the overlap of atomic wave functions, and the multipole terms U_{DD}, U_{DQ}, and U_{QQ} which are called the induced dipole-dipole, induced dipole-quadrupole, and quadrupole-quadrupole potentials, respectively. The multipole terms dominate at large separations and are fairly accurately known.[10,11]

There have been a number of recent calculations of the valence interaction U_V using the self-consistent-field (SCF) method. The work of Tapia and Bessis,[12] Tapia, Bessis, and Bratos,[13] Bender and Schaeffer,[14] and Silver and Stevens[15] has been particularly helpful in deducing the potential for intermolecular separations with $r \leq 5.5$ a.u., although there are other excellent works which give comparable results.[16] For large separations ($r \gtrsim 5.5$ a.u.), the older work of Evett and Margenau[17] (EM) seems to be the most reliable.

An alternative to calculating the four parts of the potential separately is to incorporate them into a single energy expression. The configuration interaction (CI) method is such a scheme, for which there are a variety of recent results.[18] An advantage of the CI method is that all parts of the interaction are derived from a single formalism which, in principle, is valid for all molecular separations $\vec{r}$. The major disadvantage is that a large, flexible, carefully optimized basis set of orbitals is required to obtain consistently reliable results. Moreover, the optimal set depends on the range of $\vec{r}$ investigated. Consequently, the CI calculations are presently not very accurate for $r \gtrsim 5$ a.u., whereas for $r < 5$ a.u. there seems to be general agreement between different calculations to within 10%, although their accuracy may be worse be-

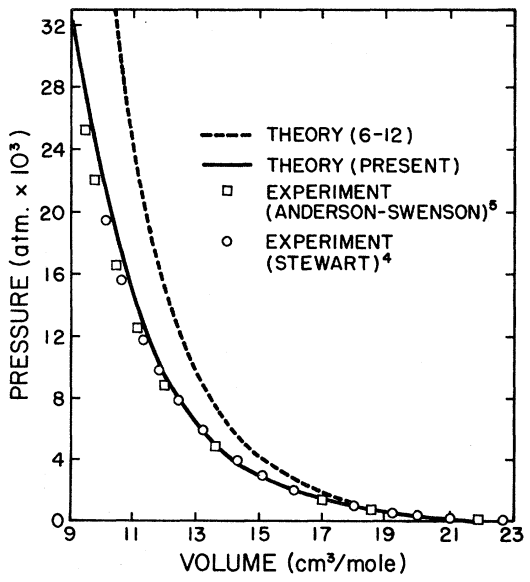

FIG. 1. Pressure vs volume for solid H_2. Theoretical and experimental results are compared.

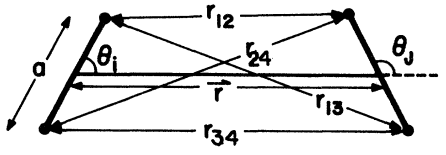

FIG. 2. Arbitrary orientation of two H_2 molecules. The intramolecular distance a is approximately 1.4 a.u.

cause all CI works suffer from similar computational limitations.

There are two major advantages to separating the potential into the valence and multipole parts. U_V can be calculated to higher accuracy, over a range of $\vec{r}$, using the SCF method, than can a CI approach with an equivalently large flexible basis set. Moreover, the multipole terms are separately known to fairly high accuracy. This means that U_V data should be more reliable at large $\vec{r}$ than are the CI results, although they too become increasingly inaccurate as $\vec{r}$ increases. The second advantage is that in the large-$\vec{r}$ region, where U_V becomes suspect, it also becomes small, and the more accurately known multipole terms begin to dominate in contribution to the total potential. This makes uncertainties in U_V at large $\vec{r}$ much less critical. The major disadvantage to separating the potential is that the multipole terms must be artificially made to vanish in the limit of small separations. That is, $U_T \simeq U_V$ as $\vec{r} \to 0$.

To calculate system properties over a wide range of conditions, there is no choice but to evaluate U_T in separate parts, which is the approach taken in this work. The alternative CI calculations are not presently capable of predicting the attractive part of the potential. To dispose of the multipole terms at small separations, we have multiplied them by the damping term

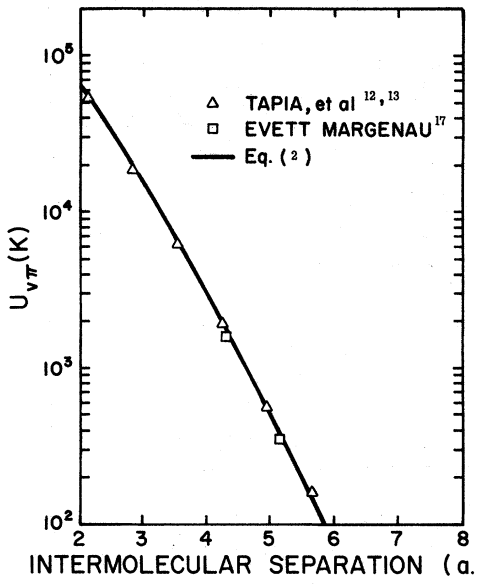

FIG. 4. Valence potential for parallel moelcular orientations at intermolecular separations $2 \leq r \leq 6$ a.u.

$$C(r) = \{1 + \exp[-4(r - 3.5)]\}^{-1}, \quad (1)$$

which ensures that $U_T \to U_V$ as $\vec{r} \to 0$. The effect is as follows: For $\vec{r} \lesssim 2.5$ a.u., $C(r) \simeq 0$, so that the dispersion terms are almost completely damped

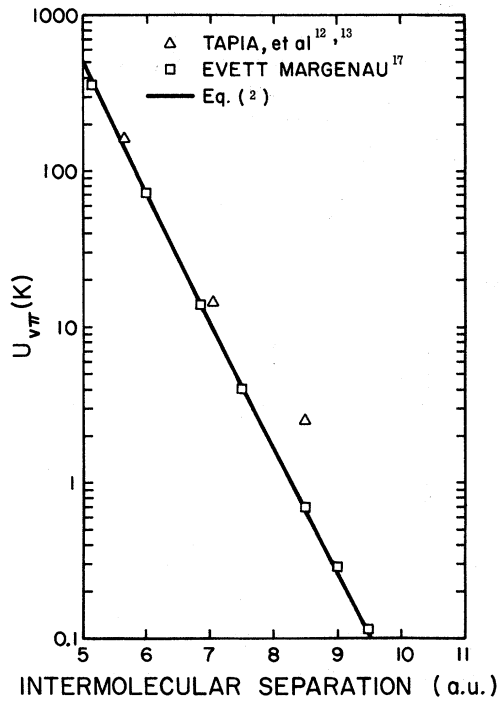

FIG. 3. Valence potential for parallel molecular orientations at intermolecular separations $5 \leq r \leq 10$ a.u.

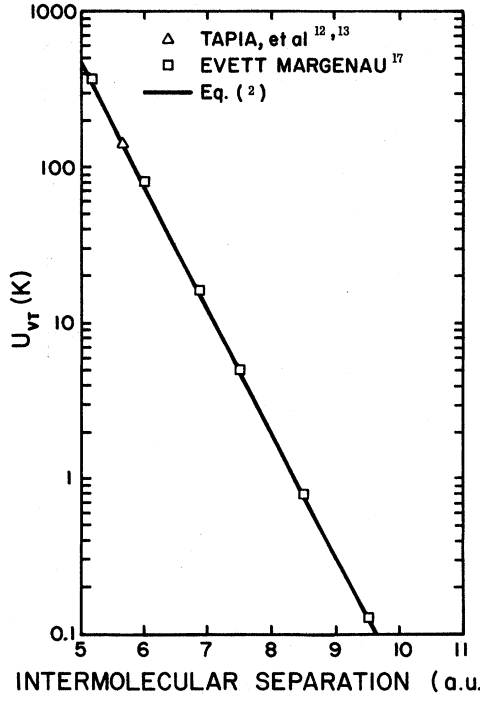

FIG. 5. Valence potential for perpenducular molecular orientations at intermolecular separations $5 \leq r \leq 10$ a.u.

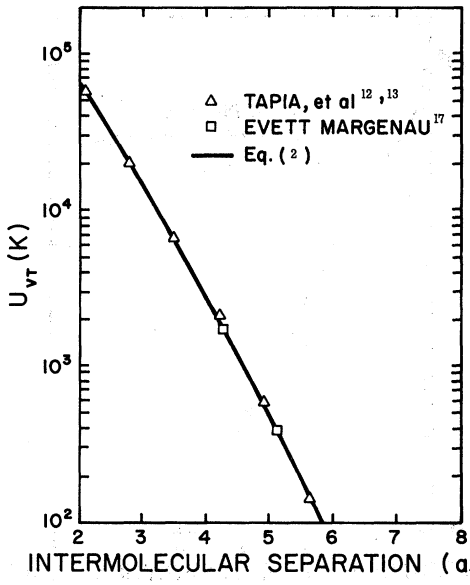

FIG. 6. Valence potential for perpendicular molecular orientations at intermolecular separations $2 \leq r \leq 6$ a.u.

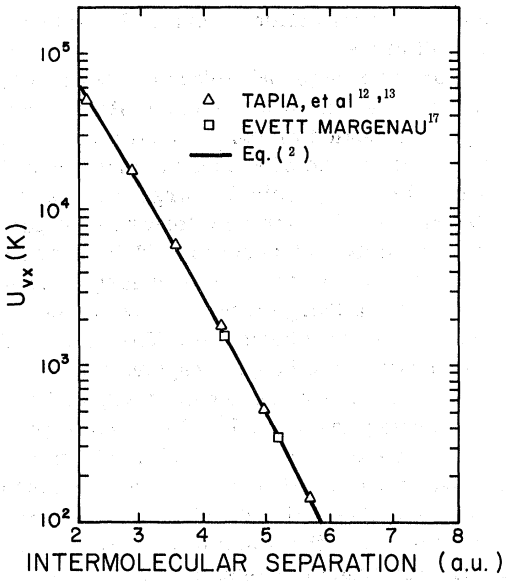

FIG. 8. Valence potential for cross-molecular orientations at intermolecular separations $2 \leq r \leq 6$ a.u.

out. Hence, $U_T \simeq U_V$. An investigation of the various atomic-orbital calculations[12-18] shows that U_T is indeed nearly equal to U_V in this regime. As $\vec{r}$ increases, $C(r)$ smoothly increases until, for $\vec{r} > 4.5$ a.u., $C(r) \simeq 1$, so that the dispersion terms are completely contained in U_T. The value of 4.5 a.u. is based upon an investigation of the range of validity of the calculational methods used to determine the multipole terms and also upon smooth extrapolations of U_T at large $\vec{r}$ to the SCF and CI values at small $\vec{r}$. The cutoff range turns out to be very close to that of Trubitsyn.[19] The uncer-

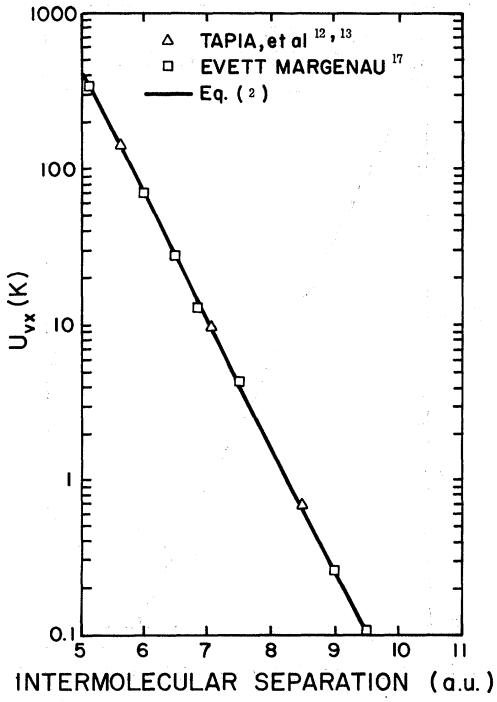

FIG. 7. Valence potential for cross-molecular orientations at intermolecular separations $5 \leq r \leq 10$ a.u.

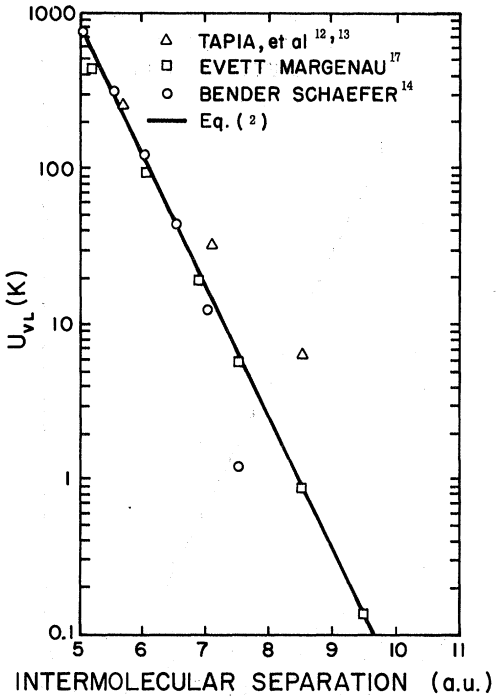

FIG. 9. Valence potential for linear molecular orientations at intermolecular separations $5 \leq r \leq 10$ a.u.

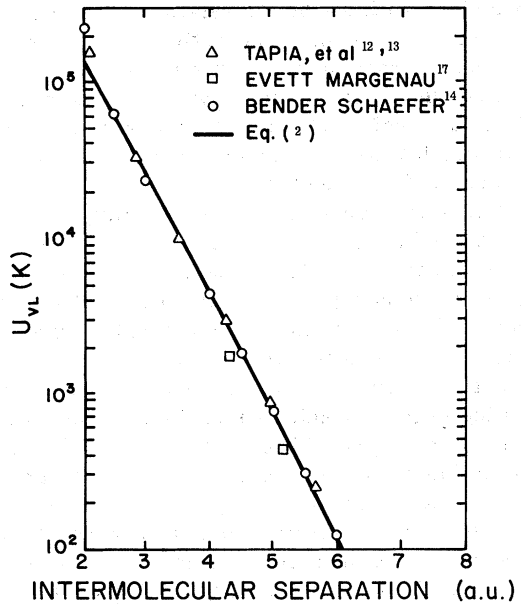

FIG. 10. Valence potential for linear molecular orientations at intermolecular separations $2 \le r \le 6$ a.u.

tainty in the potential introduced by this procedure is less than the uncertainty in the atomic-orbital data itself.

Figures 3–10 show the SCF results for the valence potential with molecular orientations (L, Π, X, T) as a function of intermolecular separation. The triangles are the recent results of Tapia, Bessis, and Bratos[13] and of Tapia and Bessis.[12] These results become increasingly suspect for intermolecular separations greater than about 5 a.u. As an example of the problem, a comparison of CI and SCF calculations by Tapia, Bessis, and Bratos[13] shows that above 5.5 a.u. some SCF results are actually lower in energy than the corresponding CI values. This is not reassuring, since the CI calculations contain the SCF part plus negative contributions from the multipole parts: hence the CI data should be consistently lower in energy. Results which show some measure of consistency for $r \gtrsim 5.5$ a.u. are those of Evett and Margenau[17] (EM), which are represented by the squares on Figs. 3–10. This work is generally regarded as among the best of the older calculations,[17] where certain approximations were made in evaluating the three- and four-center integrals. There are several less quantitative reasons for believing the EM results may be fairly reliable. In the region around $r \simeq 5$ a.u., their results seem to agree well with the more sophisticated results of Tappia and co-workers,[12,13] and for increasing r, the data fit smoothly on a semilog plot without much scatter. Also, the spherically averaged potential, deduced from the EM results, along with the multipole terms[10,11] yield a potential-well region which is quite similar to that deduced from various experimental data.[2] Nevertheless, it is apparent that more work is necessary to fully delineate the well region of the potential.

The analytic form for the data fits, exhibited as solid lines on Figs. 3–10, are

$$U_{VL} = \exp[b_L(r)], \quad U_{V\Pi} = \exp[b_\Pi(r)], \qquad U_{VT} = \exp[b_T(r)], \quad U_{VX} = \exp[b_X(r)], \tag{2}$$

where U_{VL} is the valence potential for the linear configuration, and so on. For $r < 5$ a.u.,

$$\begin{aligned} b_L(r) &= 15.4381 - 1.7532r, \\ b_\Pi(r) &= 13.8444 - 1.2827r - 0.047\,091\,6\,r^2, \\ b_T(r) &= 13.6828 - 1.105\,67r - 0.078\,402\,r^2, \\ b_X(r) &= 13.5979 - 1.154\,32r - 0.067\,37\,r^2. \end{aligned} \tag{3a}$$

For $r > 5$ a.u.,

$$\begin{aligned} b_L(r) &= 16.2815 - 1.9219r, \\ b_\Pi(r) &= 17.040\,57 - 2.291\,99r + 0.026\,851\,r^2, \\ b_T(r) &= 15.404\,74 - 1.842\,07r, \\ b_X(r) &= 15.4541 - 1.8624r. \end{aligned} \tag{3b}$$

These data only represent the interaction for four particular orientations. In order to derive a completely analytic expression for the pair potential with arbitrary relative orientations, the valence potential $U_V(r_{13}, r_{14}, r_{23}, r_{24})$ was expanded in terms of the parameter $a/2r$, where a is the distance between atoms in a given molecule (generally fixed at $a \simeq 1.4$ a.u.), and the r_{ij} are the distances between atoms of the two different molecules (see Fig. 2). The result is

$$U_V(\vec{r}, \theta_1, \theta_2, \phi) = \sum_{i=1}^{5} A_i(\vec{r}) B_i(\theta_1, \theta_2, \phi), \tag{4}$$

where the series is truncated after five terms.

Four of the functions $A_i(\vec{r})$ are chosen so that U_V *exactly* reproduces the SCF results for the four basic orientations (L, Π, T, X), as embodied in Eqs. (2) and (3). The fifth function of $\vec{r}$ was chosen such that orientations intermediate between the basic four follow the results of Silver and Stevens.[15] This condition ensures that U_V behaves properly for angular orientations other than (L, Π, T, X). The results are

$$U_T(\vec{r}, \theta_1, \theta_2, \phi) = \sum_{i=1}^{8} A_i(r) B_i(\theta_1, \theta_2, \phi); \tag{5}$$

$$A_1(r)=\exp[b_X(r)],$$
$$A_2(r)=r^2\{\exp[b_\Pi(r)]-\exp[b_X(r)]\},$$
$$A_3(r)=A_2(r)/r^2,$$
$$A_4(r)=\exp[b_T(r)]-\exp[b_X(r)]-A_2(r),$$
$$A_5(r)=2[\exp b_L(r)-\exp b_\Pi(r)]-5.4A_4(r)-4A_2(r),$$
$$A_6(r)=3.158\times10^5C(r)r^{-5},$$
$$A_7(r)=3.158\times10^5C(r)r^{-6},$$
$$A_8(r)=-3.663\times10^7C(r)r^{-8}. \quad (6)$$

The angular dependent terms B_i are

$$B_1=1,$$
$$B_2=\cos^2\theta_1+\cos^2\theta_2,$$
$$B_3=(\cos\theta_1\cos\theta_2+\sin\theta_1\sin\theta_2\cos\phi)^2,$$
$$B_4=\cos^2\theta_1+\cos^2\theta_2+0.7\cos\theta_1\cos\theta_2(\cos\theta_1\cos\theta_2+\sin\theta_1\sin\theta_2\cos\phi),$$
$$B_5=\tfrac{1}{2}\cos^2\theta_1\cos^2\theta_2,$$
$$B_6=0.048\,05[1-5(\cos^2\theta_1+\cos^2\theta_2+3\cos^2\theta_1\cos^2\theta_2)+2(\sin\theta_1\sin\theta_2\cos\phi-4\cos\theta_1\cos\theta_2)^2],$$
$$B_7=-0.2002(\sin\theta_1\sin\theta_2\cos\phi-2\cos\theta_1\cos\theta_2)^2-1.672(\cos^2\theta_1+\cos^2\theta_2)-11.133,$$
$$B_8=1.0. \quad (7)$$

The terms A_iB_i, $i=6$, 7, 8, are the quadrupole-quadrupole, dipole-dipole, and dipole-quadrupole multipole terms, respectively. Energies are in K and distances are in a.u.

A spherical average $\bar{U}_T$ can be obtained by integrating U_T over angles or, approximately, by integrating the dispersion terms and evaluating the spherical average of U_V by

$$\bar{U}_V(r)=\tfrac{1}{9}U_{VL}+\tfrac{2}{9}U_{V\Pi}+\tfrac{2}{9}U_{VX}+\tfrac{4}{9}U_{VT}. \quad (8)$$

The coefficients are the relative weights occupied by each orientation in phase space.[17] The two methods give results which agree to within 1% for all values of $\vec{r}$.

The spherical average of Eq. (5), $\bar{U}_T$, is displayed in Fig. 11 by the triangular points, and the 6-12 potential[2] is represented by the solid line. The two expressions are in fairly close agreement over the range of separations displayed. For smaller separations, however, $\bar{U}_T$ is much softer than U(6-12).

III. SOLID STATE PROPERTIES

Of principal importance in understanding solid behavior is a resolution of the large discrepancy between theory and experiment for ground-state properties, such as the PV relation.[3] As mentioned earlier, the poor theoretical results are based upon a parametrized, phenomenological potential which best reproduces experimental second-virial-coefficient data. The possibility that the theoretical description of the solid[6] or the experimental[5] data are primarily responsible for the problem have been systematically eliminated. The only remaining source of such large errors is the representation of the interaction. One possibility is that the anisotropy is more important than previously believed. It can be argued that the radial dependence, predicted from gas properties, is correct, and thus that the entire problem comes from the neglect of anisotropy. This is basically the position taken by Ebner and Sung (ES).[20] They express the potential in terms of a standard phenomenological form for the spherically symmetric part and add an anisotropic contribution which is an analytic fit of the atomic-orbital calculations of de Boer.[21] Neither the analytic fit nor the calculations of de Boer is very good in comparison to recent work.[12-18] Moreover, potentially important terms are left out of the theory, and parameters are adjusted without strong justification.

It is difficult to understand how an anisotropy which departs from sphericity by only 8% can be responsible for discrepancies between experimental PV results and theory of as much as 100% at 20 kbars, especially since the molecules are nearly free rotators at these pressures and hence their relative orientations should sample approximately

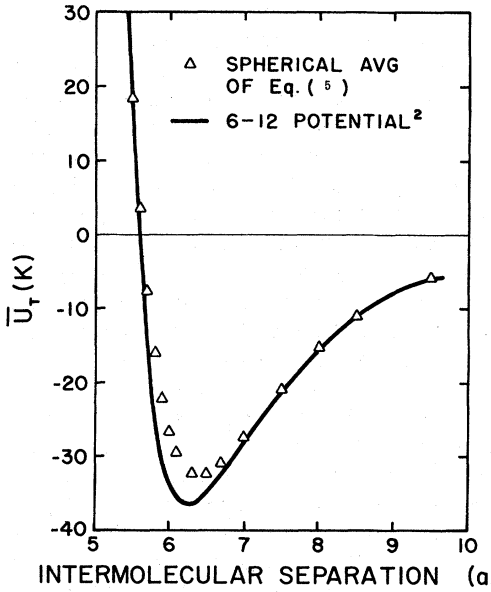

FIG. 11. The triangles are the spherical average of the anisotropic potential [Eq. (5)]. The solid line represents the 6-12 potential (Ref. 2).

equal weights in phase space. Moreover, the local field produced by near neighbors is nearly spherically symmetric.

Although the contribution of anisotropies to solid behavior is still an open question, we believe the ground-state properties are appropriately determined at low pressures from a spherically averaged potential. Based upon $\overline{U}_T(r)$, a variational, local field approximation is employed, where the trial wave function for the N-particle system is of the form

$$\Phi(\vec{r}_i, \ldots, \vec{r}_N) = \prod_{i=1}^{N} \phi(\vec{r}_i - \vec{R}_i) \prod_{i<j}^{N} f(r_{ij}), \tag{9}$$

$$\phi(\vec{r}_i - \vec{R}_i) = (\beta/\pi)^{3/4} \exp[-\tfrac{1}{2}\beta(\vec{r}_i - \vec{R}_i)^2], \tag{10}$$

$$f(r) = \exp[-\tfrac{1}{2}(\kappa/r)^5]. \tag{11}$$

The quantities β and κ are variational parameters to be determined by minimizing the energy, and $\vec{R}_i$ locates the equilibrium lattice sites. The ϕ's provide the spatial localization characteristic of a solid, and the f's account for the important short-range pair correlations. These commonly used forms are found to have sufficient flexibility to accurately represent the ground state of the system.[6] The expectation value of the Hamiltonian gives the energy

$$E = \frac{3N\hbar^2\beta}{4m} + \langle \Phi|\Phi\rangle^{-1} \sum_{\lambda<k}^{N} \int \phi^2(r_\lambda)\phi^2(r_k) f^2(r_{\lambda k}) v(r_{\lambda k}) \times G(\vec{r}_\lambda, \vec{r}_k)\, d\vec{r}_\lambda\, d\vec{r}_k, \tag{12}$$

where

$$v(r) = \overline{U}_T(r) - (\hbar^2/2m)\nabla^2 \ln f(r), \tag{13}$$

$$G(\vec{r}_\lambda, \vec{r}_k) = \prod_{s\neq\lambda,k} \int [f^2(r_{\lambda s}) f^2(r_{ks}) \phi^2(\vec{r}_s - \vec{R}_s)\, d\vec{r}_s]. \tag{14}$$

The effect of all $N-2$ molecules on an arbitrary dynamical pair (λ, k) is embodied in $G(\vec{r}_\lambda, \vec{r}_k)$. The $N-2$ molecules are said to comprise the local molecular field experienced by (λ, k). Equation (14) is an approximation which includes the direct correlations between the $N-2$ molecular-field molecules and (λ, k), but it does not contain the correlations $f(r_{ij})$ between different molecular-field molecules. In calculating H_2 properties, the product in Eq. (14) need include correlations only from the first two nearest-neighbor shells around molecules λ and k. Moreover, the exact dynamic correlations need be included only for molecules which are first-nearest neighbors to λ or k. Correlations from molecules farther than nearest neighbors away from λ or k are calculated by assuming the molecular-field molecules are static. For (λ, k) tenth-nearest neighbors or greater, sums are simply taken over a static lattice. All sums are taken over a fcc lattice except for the γ-nitrogen structure, which is tetragonal bcc. For further theoretical details, consult Ref. 22. The pressures and compressibilities are obtained by taking appropriate derivatives of the energy with respect to the volume.

A. Low-pressure results, $P \leq 2.4 \times 10^4$ atm

The calculated ground-state energy is $E_0 = -88.76 \pm 2$ K, compared with an experimental value[4] of -93.47 K, whereas the 6-12 potential gives -85 ± 2 K.[22] Figure 1 shows the pressure over the volume range $9 \leq V \leq 22.65$ cm^3/mole. The circles and squares represent the experimental data, the solid line is the result of this work, and the dashed line is the result obtained using the 6-12 potential. For molar volumes greater than about 12 cm^3/mole, the agreement with experiment is good, but for smaller volumes the comparison worsens until, at $P \simeq 2\times10^4$ atm, the calculated pressures are some 10% too high. As indicated earlier, the 6-12 potential gives pressures about 100% too high in this region.

The trial wave function used to simulate the ground state is represented by the WKB solution to the 6-12 potential for $f(r)$, Eq. (11). A more appropriate form for $f(r)$ is the WKB solution based upon $\overline{U}_T$, namely, $f(r) = \exp[-b_1 \exp(-b_2 r)]$. The total wave function then has three variational parameters, b_1, b_2, and β, which makes calculation expensive. Energies and pressures determined at three different volumes were lowered by about 5% in comparison to those obtained using Eq. (11), which improves agreement with experiment. Extensive calculations were not made, however. The data are displayed in Table I.

B. High-pressure results, $P > 2.4 \times 10^4$ atm

At high pressures, the system becomes more classical, so that unsophisticated calculational procedures[23] are adequate, although the zero-point energy is about 10% of the classical energy even at $V = 3$ cm^3/mole, a factor of 8 in compression. Also, the atomic-orbital calculations for the pair potential are more reliable[24] at small intermolecular separations, which corresponds to high pressures. However, the anisotropy becomes more pronounced, necessitating a careful treatment of the angular-dependent forces. Another difficulty, recently discussed by Ree and Bender,[25] is the likelihood that three-body forces and more become important for small intermolecular separations.

Ross[26(a)] has recently deduced a spherically averaged pair potential from atomic-orbital data,[26(b)]

TABLE I. Energy per molecule E (K), pressure and variational parameters β and κ which minimize the energy, vs molar volume. The results are based upon the spherically averaged potential $\overline{U}_T$.

	Solid H_2 (spherical average potential)			
V (cm^3/mole)	E (K/molecule)	P (10^3 atm)	β (σ^{-1})	κ (σ^{-2})
22.65	−88.75±2.1	0	15	1.11
18.00	−70.81±3.0	1.00	27	1.08
15.50	−16.05±4.5	2.49	49	1.01
13.60	59.71±5.8	4.81	55	1.01
12.00	199.11±7.2	9.42	59	1.03
10.80	386.14±10.4	16.00	70	1.00
9.00	939.04±23	32.32	80	0.97
7.50	1894.10±46	67.11	95	0.95
6.00	3906.46±84	169.20	230	0.85
5.00	6578.60±139	311.70	260	0.83
4.00	12 225.00±249	700.20	345	0.79
3.00	26 832.00±508	1920.00	400	0.75
2.00	69 419.00±1101	5580.00	550	0.61

with attractive terms added. A cell-model approximation was used to calculate PV curves. A comparison with shock-wave data indicates that the calculated pressures are too high.

We calculate high-pressure, ground-state solid properties two different ways, corresponding to extreme assumptions regarding the anisotropies. First, solid properties are calculated based upon the spherical averaged pair potential $\overline{U}_T$. A second set of calculations are performed based upon a pair potential in which the molecules are assumed to be frozen in a particular orientation. The center-of-mass motion of each molecule is treated as usual according to the theory described in the beginning of this section. The legitimacy of this latter procedure is based upon theoretical evidence[27(a)] that the molecular rotation becomes more and more hindered until, at about 3×10^5 atm, the molecules no longer rotate, but vibrate about some equilibrium orientation. Very recent calculations,[27(b)] using the accurate anisotropic potential [Eq. (5)], lead to nearly the same conclusion. With increasing pressure, the vibration about the equilibrium orientation decreases until the molecules virtually freeze in place. This phenomenon is due to the fact that the forces which orient the molecule increase faster than does the disruptive zero-point motion.

The two orientations investigated are the $P_a3(\alpha\text{-}N_2)$ and the $P4_2/mnm$ ($\gamma\text{-}N_2$) structure. The analysis is complicated because each pair of molecules having a different relative orientation interacts via a potential with different radial dependence [see Eq. (5)]. This makes summing energy contributions from different nearest-neighbor shells in Eq. (12) very complicated. Contributions from shells beyond fifth-nearest neighbors are computed using the spherical average potential. The $\gamma\text{-}N_2$ structure, which has a $P4_2/mnm$ orientation on a body-centered tetragonal lattice, is further complicated because the c/a ratio must be treated as a variational parameter for H_2. The orientational structures of nitrogen are used because N_2 is thought to be a fairly good analog for high-pressure H_2.

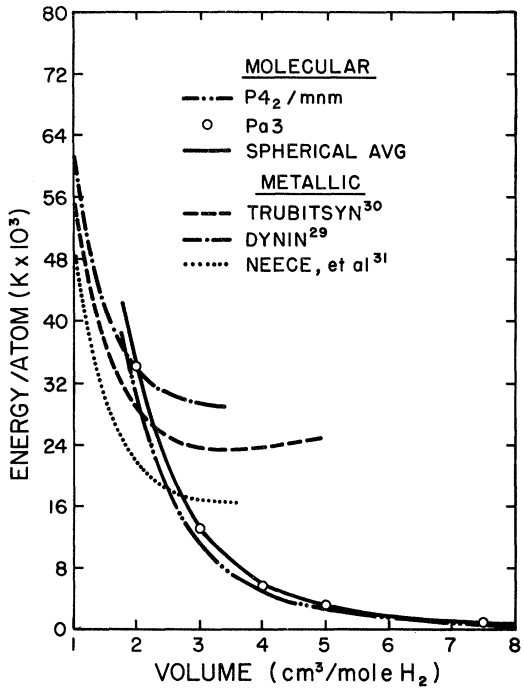

FIG. 12. Binding energy per atom vs H_2 molar volume. Results are presented for the molecular phase and for the proposed metallic phase of hydrogen.

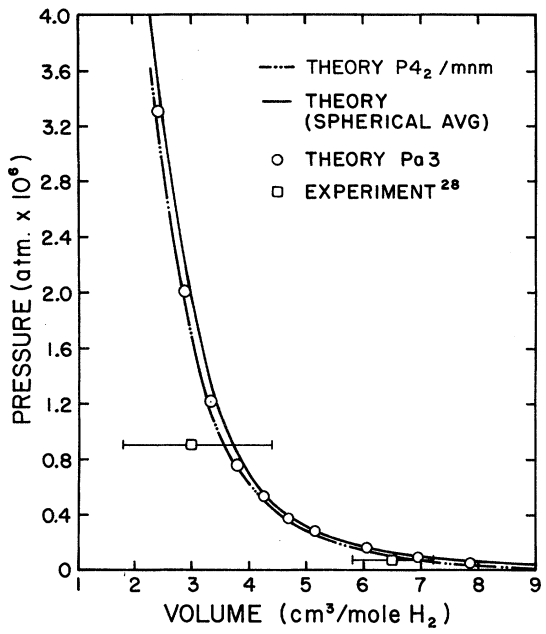

FIG. 13. Pressure vs H_2 molar volume over the range $2 \leq V \leq 9$ cm^3/mole H_2. The squares represent experimental points (Ref. 28).

The energy-volume results, bases upon $\bar{U}_T$, are represented by the solid line in Fig. 12 over the volume range $2 \leq V \leq 9$ cm^3/mole H_2. The dash–double-dot line is based upon a frozen $P4_2/mnm$ orientation, and the circles represent the P_a3 orientation. The pressures are displayed in Fig. 13 with the same format. The energies and pressures of the frozen P_a3 orientation are about 5% lower than those obtained using the spherical average potential. However, the tetragonal bcc system with $P4_2/mnm$ orientations is about (10–20)% lower in energy and pressure. The c/a ratio for this structure was taken to be 1.29, the equilibrium value for γ-N_2. This ratio should actually be treated as a variational parameter, determined by minimizing the H_2 energy. A crude analysis showed that the energy is not very sensitive to c/a in the range $1.14 \leq c/a \leq 1.41$; hence a careful minimization was not attempted. Therefore, the energies quoted for the $P4_2/mnm$ structure can be regarded as an upper limit which may be further lowered by adjusting c/a. There is no doubt that this γ-N_2 structure is preferred over the P_a3 arrangement at high pressures, as evidenced by comparing Gibbs free energies. We emphasize that results based upon frozen orientations are physically meaningless for $V > 6$ cm^3/mole because of the onset of molecular rotation.[27]

There is very little solid data at pressures greater than about 2.4×10^4 atm because of experimental difficulties. PV results are almost entirely obtained by shock-wave compression,[28] which is less reliable than the static press measurements available at low pressures.

In Fig. 13 are displayed two pressure points at about 220 kbars and at 900 kbars obtained by van Thiel *et al.*[28] The experimental uncertainties using this technique are reflected in the large error bars. The calculated PV results agree with experiment to within the over-all experimental uncertainty, although they are apparently high. The data are tabulated in Table II.

C. Insulator-metal transition

Also displayed in Fig. 12 are the energies calculated for the predicted high-pressure metallic phase of hydrogen. The results of Dynin,[29] Trubitsyn,[30] and Neece *et al.*[31] are shown as dash-dot, dashed, and dotted lines, respectively. Using the tangent-construction method, which consists of drawing a straight line that is tangent to both the molecular and the metallic curves, the pressure of the phase transition is the negative slope of that straight line. Using the metallic curve of Neece *et al.*,[31] the predicted transition pressure is $P_t \simeq 1.38 \times 10^6$ atm. Using Trubitsyn's work,[30] $P_t \simeq 2.43 \times 10^6$ atm, and for Dynin,[29] $P_t \simeq 3.32 \times 10^6$ atm. The volume changes are slightly less

TABLE II. Energy per molecule E(K), pressure, and variational parameters β and κ which minimize the energy, vs molar volume. The results are based upon Eq. (5) for the P_a3 and $P4_2/mnm$ orientations.

	P_a3 orientation (α-N_2)				$P4_2/mnm$ orientation (γ-N_2)			
V (cm^3/mole)	E (10^2 K/molecule)	P (10^3 atm)	β (σ^{-1})	κ (σ^{-2})	E (10^2 K/molecule)	P (10^3 atm)	β (σ^{-1})	κ (σ^{-2})
10.8	3.63 ± 0.41		66	1.10				
9.0	8.19 ± 0.66	23.32	78	1.05				
7.5	16.63 ± 1.95	61.01	89	0.99	12.52 ± 0.02	60.0	79	1.03
6.0		168.20			27.82 ± 0.29	142.0		
5.0	63.34 ± 2.58	301.70	280	0.86	53.63 ± 0.51	290.0	240	0.91
4.0	117.20 ± 5.00	660.20	330	0.82	105.20 ± 1.10	609.5		
3.0	259.20 ± 10.36	1820.00	375	0.72	234.90 ± 2.00	1670.0	530	0.69
2.0	662.60 ± 23.68	5400.00	500	0.60	615.90 ± 4.20	5180.0		

TABLE III. Second virial coefficients for H_2 vs temperature. $B(T)$ is the calculated result based upon the anistropic potential of Eq. (5), $\bar{B}(T)$ is the result based upon $\bar{U}_T$, B_{exp} is the experimental value (Ref. 2), B_{FL} is the result based upon the Farrar-Lee potential (Ref. 7), B_{SW} is the result based upon the shock-wave potential (Ref. 28), and B_{LJ} is the 6-12 potential result (Ref. 2).

	H_2 second virial coefficients (cm^3/mole)									
T (K)	B_{cl}	B_{1t}	B_{1r}	B_{2t}	$(C_{1p}-C_{1o})B_{1r}$	$B(T)$	$\bar{B}(T)$	B_{exp}	B_{FL}	B_{SW}	B_{LJ}
523	14.421	0.348	0.0489	−0.002	5.30×10^{-6}	14.86	14.88				
423	13.935	0.468	0.0755	−0.004	9.85×10^{-5}	14.52	14.54	16.08	19.62	10.94	16.21
373	13.477	0.559	0.0975	−0.005	4.42×10^{-4}	14.15	14.20	15.60	19.31	10.46	15.69
323	12.768	0.688	0.1302	−0.008	1.98×10^{-3}	13.59	13.65	14.87	18.79	9.75	14.92
273	11.646	0.881	0.1815	−0.013	8.87×10^{-3}	12.70	12.74	13.76	17.94	8.63	13.75
223	9.791	1.192	0.2660	−0.022	4.00×10^{-2}	11.23	11.23	11.97	16.49	6.82	11.93
173	6.479	1.762	0.4116	−0.048	1.80×10^{-1}	8.52	8.49	8.84	13.88	3.64	8.82
138	2.337	2.521	0.5690	−0.017	5.17×10^{-1}	5.22	5.06	5.01	10.60	−2.86	5.10
113	−2.545	3.492	0.6975	−0.244	1.12	1.23	1.07	.67	6.74	−5.76	0.68
98	−6.902	4.433	0.7452	−0.454	1.83	−2.39	−2.56	−3.06	3.31	−8.88	−3.16
90	−9.924	5.128	0.7359	−0.663	2.41	−4.96	−5.04				
80	−14.706	6.300	0.6433	−1.121	3.47	−9.16	−8.94				
70	−21.110	8.012	0.3555	−2.024	5.22	−15.14	−14.11				
60	−30.085	10.693	−0.4020	−3.962	8.35	−24.19	−21.30				

than one cm^3/mole H_2. These results are based upon the spherical average potential. Based upon the most stable γ-N_2 bcc orientation, the transition pressures using the different metallic results are 1.61×10^6, 2.72×10^6, and 3.76×10^6 atm, in the same order as presented above. Contrary to prevailing impressions, uncertainties in the metallic phase are a major source of uncertainty in predicting the phase transition pressure.

IV. SECOND VIRIAL COEFFICIENTS

Calculations of second virial coefficients $B(T)$ for atomic and molecular systems have been almost exclusively based upon a spherically symmetric representation of the pair potential. Wigner and Kirkwood[32] showed that $B(T)$ can be expressed as an expansion in powers of h. The explicit forms are well documented.[33] For systems with anisotropic interactions, such as diatomic gases, Wang Chang[34] has modified the Wigner-Kirkwood power-series expansion to accommodate the angular dependence of the potential. The effect of discrete molecular rotational states is also incorporated. Although some attempts have been made to calculate $B(T)$ using this method, the phenomenological forms chosen to represent the anisotropy are not satisfactory.

TABLE IV. Second virial coefficients for D_2 vs temperature. $B(T)$ is the calculated result based upon the anistropic potential of Eq. (5), B_{exp} is the experimental value (Ref. 2), B_{LJ} is calculated from the 6-12 potential, $B_{H_2}-B_{D_2}$ is the difference in $B(T)$ between H_2 and D_2, and $(B_{H_2}-B_{D_2})_{exp}$ is the experimental value for this difference (Ref. 2).

	D_2 second virial coefficients (cm^3/mole)									
T (K)	B_{cl}	B_{1t}	B_{2t}	B_{2t}	$(C_{1p}-C_{1o})B_{1r}$	$B(T)$	B_{exp}	B_{LJ}	$B_{H_2}-B_{D_2}$	$(B_{H_2}-B_{D_2})$
523	14.421	0.174	0.0241	-0.560×10^{-3}		14.619			0.189	
423	13.935	0.234	0.0368	-0.970×10^{-3}		14.205	15.54	15.87	0.260	0.54
373	13.477	0.280	0.0474	-0.136×10^{-2}		13.803	15.07	15.33	0.313	0.53
323	12.768	0.344	0.0631	-0.201×10^{-2}		13.173	14.38	14.53	0.388	0.49
273	11.646	0.441	0.0880	-0.317×10^{-2}	0.519×10^{-5}	12.171	13.30	13.34	0.500	0.46
223	9.791	0.597	0.1310	-0.554×10^{-2}	0.105×10^{-3}	10.513	11.53	11.45	0.681	0.44
173	6.479	0.882	0.2145	-0.119×10^{-1}	0.198×10^{-2}	7.553	8.37	8.20	0.985	0.47
138	2.337	1.261	0.3302	-0.268×10^{-1}	0.156×10^{-1}	3.881	4.38	4.29	1.340	0.63
113	−2.545	1.747	0.4774	−0.061	0.688×10^{-1}	−0.439	−0.38	−0.30	1.672	1.05
98	−6.902	2.218	0.6135	−0.114	0.168	−4.256	−4.59	−4.35	1.865	1.53
90	−9.924	2.566	0.7081	−0.166	0.271	−6.901			1.935	
80	−14.706	3.152	0.8549	−0.280	0.495	−11.081				
70	−21.110	4.009	1.0395	−0.506	0.912	−16.693				
60	−30.085	5.350	1.2601	−0.991	1.715	−24.465				
50	−43.476	7.673	1.4695	−2.154	3.383	−36.685				

As a result, it is not known to what extent the anisotropy contributes to the second virial coefficients for H_2. However, the relatively accurate representation of the anisotropy given by Eqs. (3) and (5)–(7) makes it possible to partially resolve that uncertainty. Before describing the calculations, some insight into the problem is gained from general considerations. Second virial coefficients and most transport properties are intimately related to the dynamics of two-body collision processes. An inspection of Eq. (5) shows that the interaction between two H_2 molecules can be very different, depending on their relative orientation; hence a description of the relative molecular orientations during the collision period is essential. If the rotational period τ_r is small compared to the collision period τ_c over which the interaction is effective, the pair experiences many different relative orientations during a single collision. This condition must be accounted for in calculating physical properties. For $\tau_r \ll \tau_c$, it may be acceptable to represent the interaction by the potential averaged over all orientations. If $\tau_r \gg \tau_c$, the molecular orientations are spatially frozen during the collision and can be deduced from the dynamical trajectories. The situation is most complicated when $\tau_r \simeq \tau_c$.

A. The Wang Chang method

The second virial coefficient for a diatomic gas is given by the series

$$B(T) = B_{\rm cl} + B_{1t} + B_{1r} + B_{2t} + B_{2r} + \cdots + B_0, \quad (15)$$

where $B_{\rm cl}$ is the classical term, B_{1t} and B_{2t} are the first two quantum corrections owing to translational degrees of freedom, B_{1r} and B_{2r} are the quantum corrections arising from the rotational degrees of freedom, and B_0 is the statistical correction. These four-dimensional integrals which depend upon r, θ_1, θ_2, and $\phi_1 - \phi_2$ are given in Refs. 33 and 34.

The results for the second virial coefficients of H_2 and D_2, using Eq. (15), are tabulated in Tables III and IV and displayed in Figs. 14 and 15. Also tabulated are the results for H_2, based upon a spherical average of $U_T(r, \theta_1, \theta_2, \phi)$ and including the first two quantum corrections as well as the statistical term. A comparison of these results with those obtained using the Wang Chang formalism directly measures the impact of the potential anisotropy on second virial coefficients. As can be seen from Table III and Fig. 14, the difference in $B(T)$ derived using these two methods is small. It would appear that the anisotropy does not contribute to $B(T)$ in an important way. At low temperatures ($T \lesssim 80$ K) one cannot draw this conclusion, because the approximate expressions used here to calculate $B(T)$ are no longer reliable.

We have also calculated virial coefficients for several potentials deduced from various experimental data. As mentioned earlier, Farrar and Lee[7] have unfolded a spherically symmetric potential from H_2-H_2 scattering results which well represents that data. Figure 14 shows that $B(T)$ calculated from this potential is in poor agreement with experiment. This was anticipated by Farrar and Lee.

Another potential form has been derived from the PV, shock-wave data of van Thiel *et al.*[28] Figure 14 shows that virial coefficients calculated from this potential are not in good agreement with experiment either. The triangles in Fig. 14 represent $B(T)$ for the Lennard-Jones 6-12 potential with parameters $\epsilon = 36.7$ K and $\sigma = 2.958$ Å, which are so chosen because they give the best fit to the experimental virial coefficient data.[2]

Figure 16 shows the difference in $B(T)$ between hydrogen and deuterium, designated by the solid

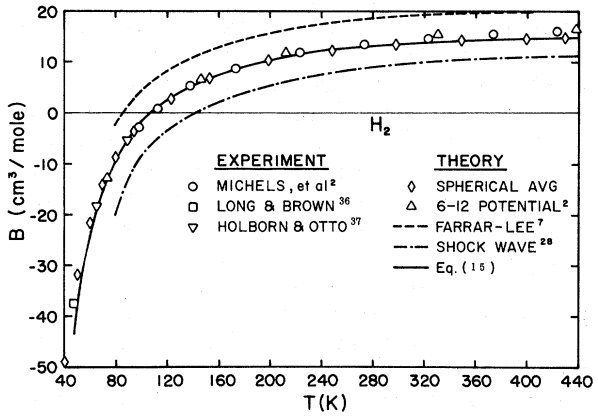

FIG. 14. Second virial coefficient vs temperature for H_2.

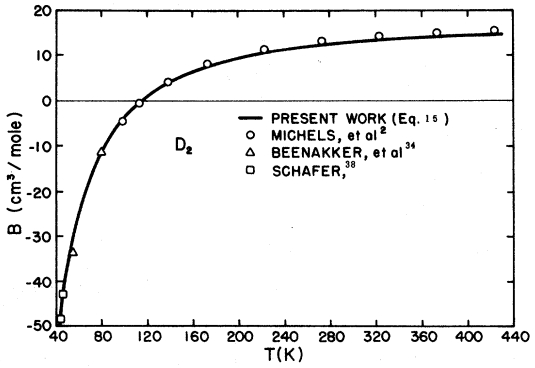

FIG. 15. Second virial coefficient vs temperature for D_2.

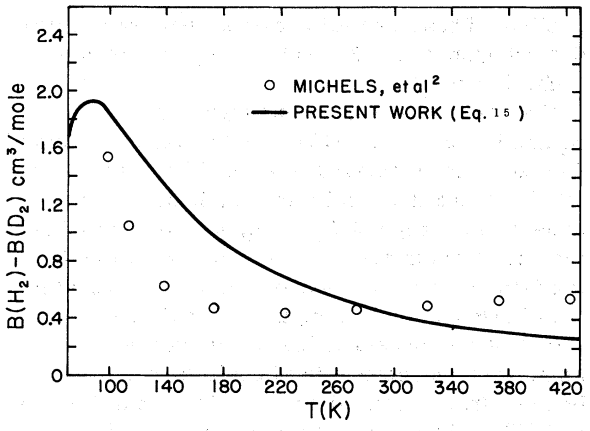

FIG. 16. Difference between H_2 and D_2 second virial coefficients vs temperature.

line. The data points are the experimental work of Michels *et al.*[2] We believe the turnover in the calculated difference is a reflection of the increasing inaccuracy of the theory at low temperatures. The difference in $B(T)$ between para- and ortho-hydrogen is displayed for H_2 and D_2 in Fig. 17. Experimental data sufficiently accurate to measure $B_p - B_o$ exists only at temperatures below that for which the theory is valid.

V. DISCUSSION AND CONCLUSIONS

The ground-state energy, PV data, and other related properties of solid H_2 have been predicted to within 10% of experiment over the pressure range $0 \leq P \leq 2.4$ kbars, based upon the spherical average of an analytic, anisotropic interaction deduced from SCF and perturbation calculations.

A satisfactory potential should yield good predictions for other H_2 properties, as well as for the solid. Hence, second virial coefficients $B(T)$ have been calculated for H_2 and D_2 over the temperature range $60 \lesssim T \leq 523$ K. It was not previously known if it is appropriate to calculate $B(T)$ from a spherically averaged potential or from a fully anisotropic representation. To resolve this question, the $B(T)$ were first calculated from $\overline{U}_T$, used in the solid description; then, in a second calculation, the full anisotropies were incorporated using the method of Wang Chang.[34] The two methods give nearly identical results, indicating that the anisotropies contribute little to $B(T)$. The $B(T)$ for both H_2 and D_2 compare closely with experiment for $T < 225$ K, but as T approaches 432 K, they disagree by nearly 10%. The overall agreement is, however, much better than that generally obtained using phenomenological potentials deduced from other H_2 properties.

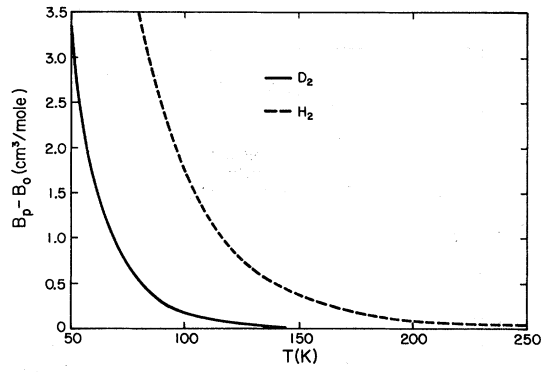

FIG. 17. Difference in second virial coefficients between ortho- and para-H_2 vs temperature. The solid line displays the same difference for D_2.

It is evident that all calculated system properties agree with experiment to within 10% and, in most cases, better than that. Preliminary results for the differential and total cross sections, based upon $\overline{U}_T$, also support this claim. In view of the fact that the calculations are from first principles and contain no adjustable parameters, the agreement is satisfactory.

There is no evidence that anisotropies have any major effect on any H_2 properties studied here, except at very high pressures. Calculations of transport properties, in addition to a complete anisotropic description of the solid, are necessary to more fully understand the impact of angular-dependent forces.

Understanding high-pressure behavior is complicated by the fact that experimental evidence is sparse, relatively unreliable, and because there is evidence that three- or more-body forces may be important. Ree and Bender[25] have carried out CI and SCF calculations for pairs of H_2 molecules and for groups of three as a function of intermolecular separation. They find that the assumption of pairwise additivity seems to break down at small $\vec{r}$. The violation apparently becomes very serious for separations less than 3.5 a.u. As can be seen from Fig. 12, the H_2 energy-volume curve must be known to volumes at least as low as 3 cm^3/mole (a nearest-neighbor distance of 3.61 a.u.) in order to make an accurate tangent construction for the metallic transition pressure and volume change. This is in the region where three-body contributions are beginning to become important.

Although attention has been focused on an important problem for systems at high pressure, we believe it is premature to conclude that many-body forces are necessary in predicting the metallic-hydrogen transition pressure. The accuracy of existing atomic-orbital calculations, especially three-body results, may not be good enough. It is

also a concern that only limited orientations of three molecules have been calculated and used in analysis. This is clearly pointed out by Ree and Bender. Finally, the comparison of the Ree-Bender results with shock-wave data is not convincing in view of the very large uncertainties in the experiment. In fact, the relatively hard, spherically averaged potential deduced in this work gives pressures which fall within the experimental error flags (see Fig. 13). Historically, calculations of many-body contributions have been very difficult to interpret because of the computational problems inherent in the work.[10] It may be that three-body terms are fully as important as indicated by Ree and Bender, but much more work is necessary to convincingly delineate the situation.

Regardless of uncertainties over many-body forces, a prediction of the high-pressure equation of state, based upon an accurate pair potential, is a necessary element in the evolution of the problem and must precede definitive understanding of three-body effects. Based upon Ree and Bender's results, we estimate that the neglect of three-body forces introduces uncertainties of about 10% in the equation-of-state calculations at 3 cm^3/mole, although Ree and Bender's estimate is larger. This seems to be acceptable at present, in view of other uncertainties previously discussed. Our results clearly indicate that the bcc γ-N_2 structure is energetically favored over the fcc α-N_2 structure at high pressures. The predicted metallic transition pressures range from 1.61×10^6 to 3.76×10^6 atm, depending on which metallic results are used.

ACKNOWLEDGMENT

One of us (R. D. E.) wishes to express appreciation to the Aspen Center for Physics, where some of this work was completed.

---

*Work supported by NASA Grant No. NGL 06-002-159.

[1]W. Kolos and C. C. J. Roothaan, Rev. Mod. Phys. 32, 219 (1960).

[2]A. M. Michels, W. de Graff, and C. A. ten Seldam, Physica (Utr.) 26, 393 (1960).

[3]T. A. Bruce, Phys. Rev. B 5, 4170 (1972); J. A. Krumhansl and S. Wu, Phys. Lett. 28A, 263 (1968); R. D. Etters and R. L. Danilowicz, Phys. Rev. A 9, 1698 (1974).

[4]J. W. Stewart, J. Phys. Chem. Solids 1, 146 (1956).

[5]M. S. Anderson and C. A. Swenson, Phys. Rev. B 10, 5184 (1974).

[6]J. P. Hansen and D. Levesque, Phys. Rev. 165, 293 (1968). See also Ref. 3.

[7]J. M. Farrar and Y. T. Lee, J. Chem. Phys. 57, 5492 (1972).

[8]W. England, R. Etters, J. Raich, and R. Danilowicz, Phys. Rev. Lett. 32, 758 (1974).

[9]The spherically averaged pair potential deduced in Ref. 8 is slightly different from the present result because some recent atomic-orbital data was not used earlier. This accounts for minor differences in predicted solid properties. Also, because no completely analytic, anisotropic potential form was then available, the spherical average was obtained using approximate methods. The second virial coefficient, deduced in Ref. 8 from a spherically averaged potential, is incorrect because of a mathematical error. Hence, conclusions about the importance of anisotropies, based upon that particular curve, are invalid.

[10]H. Margenau and N. R. Kestner, *Intermolecular Forces*, 2nd ed. (Pergamon, New York, 1971).

[11]G. A. Victor and A. Dalgarno, J. Chem. Phys. 53, 1316 (1970).

[12]O. Tapia and G. Bessis, Theor. Chim. Acta 25, 130 (1972).

[13]O. Tapia, G. Bessis, and S. Bratos, Int. J. Quantum. Chem. Symp. 4, 289 (1971).

[14]C. F. Bender and H. F. Schaefer, III, J. Chem. Phys. 57, 217 (1972).

[15]D. M. Silver and R. M. Stevens, J. Chem. Phys. 59, 3378 (1973).

[16]C. F. Bender, H. F. Schaefer, and P. A. Kollman, Mol. Phys. 24, 235 (1972); V. Magnasco and G. F. Musso, J. Chem. Phys. 46, 4015 (1967); 47, 1723 (1967).

[17]A. A. Evett and H. Margenau, Phys. Rev. 90, 1021 (1953).

[18]C. W. Wilson, Jr., and W. A. Goddard, III, J. Chem. Phys. 51, 716 (1969); M. Rubinstein and I. Shavitt, J. Chem. Phys. 51, 2014 (1969); A. Williams, MIT Solid State and Molecular Theory Group, Quarterly Progress Report No. 46 (1962), p. 150.

[19]V. P. Trubitsyn, Fiz. Tverd. Tela 7, 3363, 3443 (1965) [Sov. Phys. Solid State 7, 2708, 2779 (1965)].

[20]C. Ebner and C. C. Sung, Solid State Commun. 11, 489 (1972).

[21]J. de Boer, Physica (Utr.) 9, 363 (1942).

[22]R. D. Etters and R. L. Danilowicz, Phys. Rev. A 9, 1698 (1974).

[23]R. D. Etters, J. C. Raich, and D. Chand, J. Low Temp. Phys. 5, 711 (1971).

[24]A. K. McMahan, H. Beck, and J. A. Krumhansl, Phys. Rev. A 9, 1852 (1974).

[25]F. H. Ree and C. F. Bender, Phys. Rev. Lett. 32, 85 (1974).

[26](a) M. Ross, J. Chem. Phys. 60, 3634 (1974); (b) C. F. Bender (unpublished).

[27]J. C. Raich and R. D. Etters, J. Low Temp. Phys. 6, 229 (1972); (b) W. England, J. Raich, and R. D. Etters (unpublished).

[28]M. van Thiel, M. Ross, B. L. Hord, A. C. Mitchell, W. H. Gust, M. J. D'Addario, and R. N. Keeler, Phys. Rev. Lett. 31, 979 (1973); M. Ross, J. Chem. Phys. 60, 3634 (1974).

[29]E. A. Dynin, Fiz. Tverd. Tela 13, 2488 (1971). [Sov. Phys. Solid State 13, 2089 (1972)].

[30]V. P. Trubitsyn, Fiz. Tverd. Tela 7, 3363, 3443 (1965)

[Sov. Phys. Solid State 7, 2708, 2779 (1966)].
[31]G. A. Neece, F. J. Rogers, and W. G. Hoover, J. Comput. Phys. 7, 621 (1971).
[32]E. Wigner, Phys. Rev. 40, 749 (1932); J. G. Kirkwood, Phys. Rev. 44, 31 (1933).
[33]J. O. Hirschfelder, C. F. Curtiss, and R. B. Bird, *Molecular Theory of Gases and Liquids* (Wiley, New York, 1954).
[34]C. S. Wang Chang, Ph.D. thesis (University of Michigan, 1944) (unpublished).
[35]E. A. Long and O. L. I. Brown, J. Am. Chem. Soc. 59, 1922 (1937).
[36]L. Holborn and J. Otto, Z. Phys. 23, 77 (1924); 30, 320 (1924); 33, 1 (1925); 38, 359 (1926).
[37]K. Schafer, Z. Phys. Chem. B 36, part 2, 85 (1938).
[38]F. H. Varekamp and J. J. M. Beenakker, Physica. Grav. 25, 889 (1959).